UDC 531.76+534.134+534.141.2 DOI: 10.18698/0236-3941-2021-1-103-113

EVALUATION OF THE COMPOSITE BARRIER NATURAL OSCILLATIONS INFLUENCE ON THE GENERATED SHOCK LOADING

A.S. Borozenets
A.V. Proskurin
A.V. Shlishevskiy niik@vniitf.ru

Federal State Unitary Enterprise "Russian Federal Nuclear Center — Zababakhin All-Russia Research Institute of Technical Physics", Snezhinsk, Chelyabinsk Region, Russian Federation

Abstract

The problem of studying behavior of various structures under the influence of intense impulsive (shock) loads arising during operation of many modern facilities, machines and devices remains relevant for many years. Shock loading in laboratory conditions is generated due to interaction between the test object and the braking device (barrier). In this case, braking device or barrier could be a one-piece or a prefabricated structure. If the braking device (barrier) dimensions commensurate with the test object, the braking device natural oscillation frequencies excited during interaction between the test object and the braking device (barrier) could be found in the range of the test object natural oscillation frequencies. Frequency determination within the signal spectrum registered on the test object and caused by oscillations of the braking device (barrier) or test equipment, would assist in better assessing the test object shock loading and its compliance with real operating conditions

Keywords

Reinforced concrete barrier, shock loading, longitudinal oscillations, piezo accelerometer, digital filtering, spectral density

Received 22.08.2020
Accepted 29.09.2020

Introduction. Shock loading [1–3] in laboratory testing could be set in the form of collision conditions (drop height, approach speed) [4–6], or in the form of impact impulse parameters (amplitude and duration of impact acceleration) [7, 8]. In the first case of setting the shock loading in the form of implementing the collision conditions, test equipment as it is misses, and a test object (TO) stays in conditions as close as possible to the real ones. However, the real (semi-infinite) barrier in this case is replaced by a composite barrier, i.e., a barrier possessing its natural oscillation frequencies. In the second

case, loading conditions are set in the form of impact impulse parameters. With this approach, intermediate elements in the form of test equipment are positioned between the TO and the braking device, and they have their individual set of natural vibration frequencies. In addition, the braking device has its own set of natural frequencies. Obviously, when analyzing results of a TO shock loading, it is necessary to evaluate natural oscillation frequencies of composite obstacles, test equipment or braking devices in order to assess these elements oscillation influence on the TO shock loading.

Works [7, 8] present studies of shock loading set in the form of its parameters. The main drawback of these works is that influence of the test equipment natural oscillation frequencies on the generated shock loading is not being assessed, which in some cases could provoke a significant error in estimation of the TO reaction during the impact testing. This article is devoted to assessing the influence of composite barrier oscillations on accelerations of the TO interacting with it.

Impact testing. TO 4 m long was exposed to shock loading. The load was generated due to interaction between the TO and the barrier, which appeared to be a structure made of reinforced concrete blocks with internal reinforcement (Fig. 1).

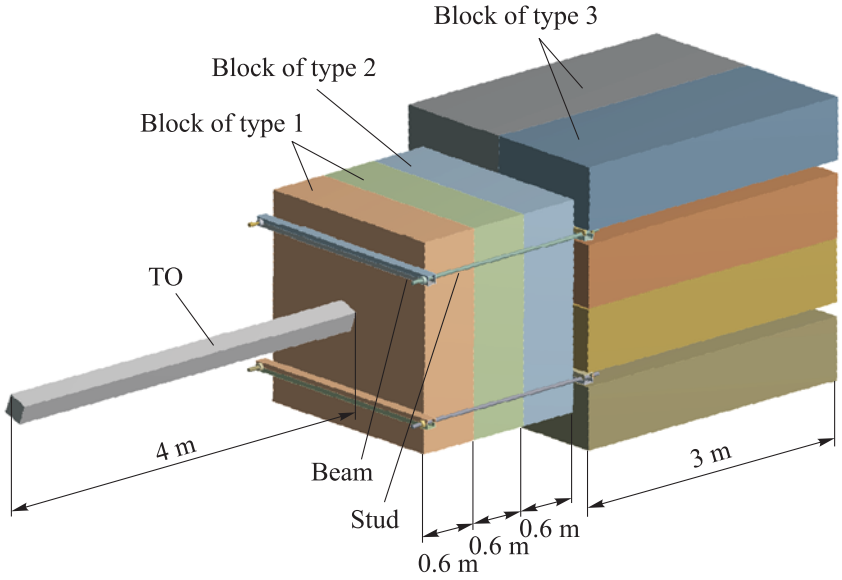

Fig. 1. Barrier external appearance

Table 1 presents physical and mechanical characteristics of the barrier element materials [9–12], as well as longitudinal dimensions (thickness and length) for blocks of types 1, 2 and 3.

Table 1

Physical and mechanical characteristics of the barrier element materials

Element	Material	E, MPa	ρ, kg/m^3	μ	a, m/s^2	h (l), m
Block of type 1	M400 concrete	$3.25 \cdot 10^4$	2170	0.18	4487* (4750)*	0.6
Block of type 2	M300 concrete	$3 \cdot 10^4$	2183	0.18	4200*	0,6
Block of type 3	M300 concrete	$3 \cdot 10^4$	2183	0.18	4200*	3
TO	Steel	$2 \cdot 10^5$	7850	0.3	5200	4

* Speed of sound determined experimentally (speed of sound value in second block of type 1 is provided in brackets).

To register accelerations near the TO end face opposite to the impact zone, four piezo accelerometers (PMT — primary measurement transducer) were installed with symbols 1X, 2X, 3X and 4X of the AP11 type (conversion coefficient 11 ± 4 pC/g, registered acceleration amplitude up to 5000 g, operating frequency range 2–15 000 Hz) for VGO-1 adhesive sealant. Signal registration from piezo accelerometers was carried out using the PARUS 01.01.000 autonomous registration device designed and developed by the FTI UB RAS, Izhevsk (shock resistance up to 100 000 m/s^2; number of channels is 4; registration time is 4, 8, 16 and 32 s, upper cutoff frequency is 55 000 Hz, sampling frequency is 120, 60, 30 and 15 Hz).

Signals registered by piezo accelerometers are shown in Fig. 2. The A peak acceleration values and the τ acceleration pulse duration for each piezo accelerometer signal (see Fig. 2) are presented in Table 2. Besides, average values of these A_{av} and τ_{av} parameters are provided there. Signal spectral densities [13] shown in Fig. 2 are provided in Fig. 3.

To detail the graphs of spectral densities, let us exclude from consideration the range from 0 to 77 Hz, which characterizes shock loading with the 13 ms pulse duration ($f_{\text{imp.load}} = 1/\tau_{av} = 1000/13 = 77$ Hz). Detailed graphs of the signal spectral density registered by 1X, 2X, 3X and 4X piezo accelerometers in the 77–2000 Hz range are shown in Fig. 4.

Values of the spectral density peak frequencies pertaining to the 1X, 2X, 3X and 4X piezo accelerometer signals in the 77–2000 Hz frequency range are given in Table 3. Only those peaks were considered, which amplitudes corresponded to the $A > 0.1A_{\max}$ condition, where $A_{\max}$ is the maximum peak amplitude.

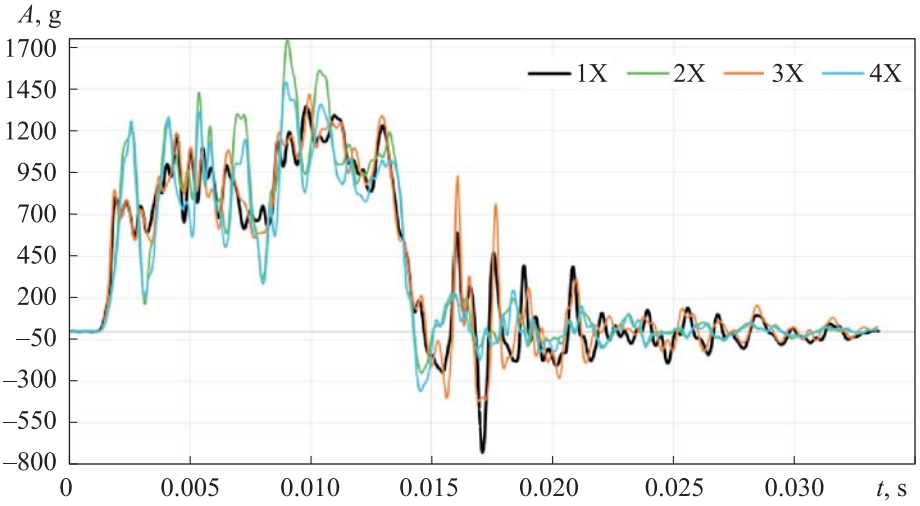

Fig. 2. Graphs of registered impact accelerations

Table 2

Impact acceleration signal parameters

Primary measurement transducer	A, g	A_{av}, g	τ, ms	τ_{av}, ms
1X	1348	1500	13	13
2X	1750		12.5	
3X	1414		13	
4X	1486		12.5	

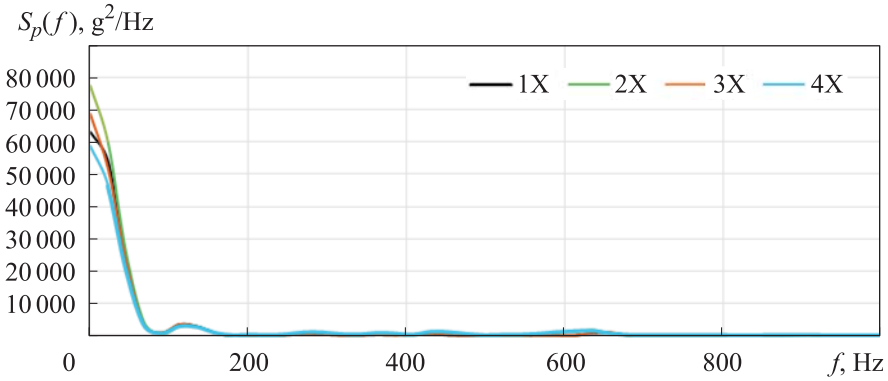

Fig. 3. Graphs of the registered impact accelerations spectral density

Computational study. Let us consider the barrier blocks and the TO as a set of rods with different lengths.

As is known from work [14], longitudinal oscillation frequencies of a rod with free ends are determined by the following formula:

$$f_i = \frac{ai}{2l}, \quad i = 1, 2, 3, \ldots \text{ is an integer,} \tag{1}$$

where l is the rod length; a is the wave speed in the rod. Let us restrict ourselves to considering only the first oscillation modes, i.e., by the $i = 1$ case.

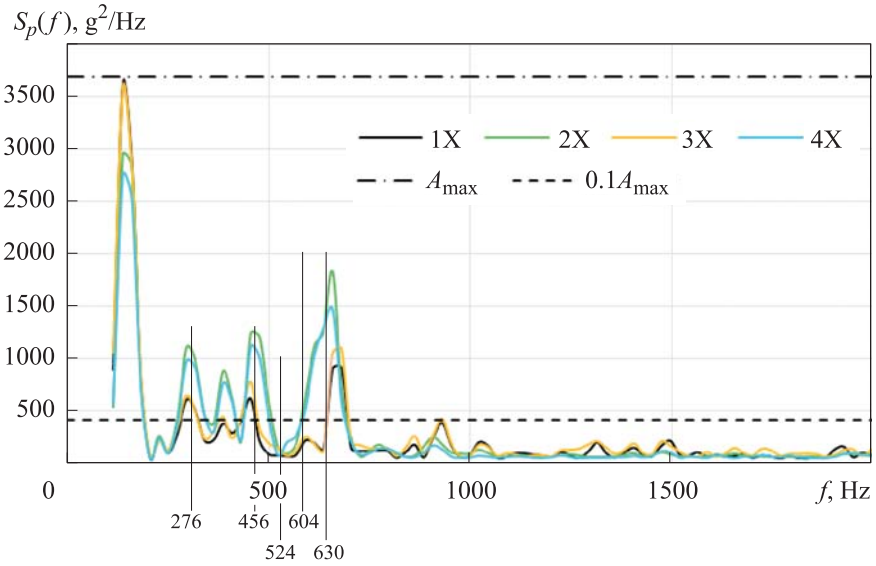

Fig. 4. Spectral density of signals registered by piezo accelerometers

Table 3

Piezo accelerometer signal spectral density peak frequencies

Primary measurement transducer	Frequency value, Hz				
1X	114	272	364	431	657
2X	114	273	363	440	634
3X	113	272	363	431	658
4X	114	273	363	431	634
Average frequency value	113.8	272.5	363.3	433.3	645.8

When a composite barrier is excited, the shock wave propagates and entrains elements of the barrier into the oscillatory process. The wave divides at the barrier element boundary into reflected and passing waves. Reflected wave moves in the opposite direction to the original motion direction. The passing wave continues to move in the original direction until the next boundary. Thus, the distance to the boundary of any barrier element determines the l length of a conventional rod, which is used to identify the longitudinal oscillation frequency according to (1). The first boundary in the collision scheme shown in Fig. 1 lies

between the TO and the face side of the first block of type 1. Thus, the highest frequency of longitudinal oscillations would be determined by the TO dimensions. The distance to the number 1 boundary is determined by the TO length. Boundary number 2 stays between the back side of the first block of type 1 and the front side of the second block of type 1. Distance to boundary number 2 is determined by the total of the TO length and the thickness of block of type 1. Distances to other boundaries are determined in the same way. Table 4 provides the numbers of boundaries that determine the barrier oscillation natural frequencies, barrier composite elements, which dimensions indicate the distance to these boundaries, and the *l* parameter value for these boundaries.

Table 4

Barrier boundary numbers and elements, which dimensions determine the distance to the boundary

Boundary number	Composition	*l*, m	Frequency, Hz
1	TO	4	630
2	TO + Block of type 1	4.6	604
3	TO + two Blocks of type 1	5.2	524
4	TO + two Blocks of type 1 + Block of type 2	5.8	456
5	TO + two Blocks of type 1 + Block of type 2 + Block of type 3	8.8	276

Oscillation frequency determined by boundary number 1 depends on the wave motion speed along the TO. Then, let us consider TO as a steel rod, apply formula (1) to the boundary number 1, and find the highest frequency of longitudinal oscillations:

$$f_1 = \frac{a_1}{2l_1} = \frac{\sqrt{E/\rho}}{2l_1} = \frac{\sqrt{(2\cdot 10^{11})/7850}}{2\cdot 4} = 630 \text{ Hz},$$

where a_1 is the wave speed in TO; l_1 is the TO length.

Let us consider the following boundaries. Common to the boundaries numbers 2–5 is the fact that wave motion to these boundaries occurs along the barrier constituent elements with different speeds determined by these constituent element properties. It follows from (1) that the longitudinal oscillation frequency is determined by the time of wave passing along the rod [14]. Thus, longitudinal oscillation frequencies determined by boundaries numbers 2–5 could be found by the following formula:

$$f = \frac{1}{T} = \frac{1}{\sum\limits_{k=1}^{N} \frac{2l_k}{a_k}}, \qquad (2)$$

where T is the oscillation period; a_k is the wave speed in the k-th barrier component; l_k is the length of the k-th barrier component; N is the boundary number.

Let us present several comments on the speed of wave propagation in reinforced concrete barriers. The best option is to use the wave speed values in reinforced concrete block obtained experimentally, since the type of internal reinforcement would affect the wave propagation speed. In the absence of experimental data, it is preferable to use the speed of elastic wave propagation in the continuous medium [15]:

$$a = \sqrt{\frac{E(1-\mu)}{(1+\mu)(1-2\mu)\rho}} = \sqrt{\frac{3.25 \cdot 10^{10}(1-0.18)}{(1+0.18)(1-2 \cdot 0.18) \cdot 2170}} = 4033 \text{ m/s},$$

where E is the material elasticity modulus; μ is Poisson's ratio; ρ is the material density rather than the speed of elastic wave propagation in the rods:

$$a = \sqrt{\frac{E}{\rho}} = \sqrt{\frac{3.25 \cdot 10^{10}}{2170}} = 3870 \text{ m/s}.$$

Using expression (2), let us determine the first natural frequency of longitudinal oscillations for boundary number 2:

$$f_2 = \frac{1}{\frac{2l_1}{a_1} + \frac{2l_2}{a_2}} = \frac{1}{\frac{2 \cdot 4}{\sqrt{(2 \cdot 10^{11})/7850}} + \frac{2 \cdot 0.6}{4487}} = 604 \text{ Hz}.$$

Oscillation frequencies for boundaries numbers 3–5 are determined in the same way. Calculation results are provided in Table 4. Values of the calculated frequencies obtained are plotted in Fig. 4 as vertical lines.

Let us compare calculated values of the composite barrier longitudinal oscillation frequencies and average values of frequency peaks in the piezo accelerometer signal spectral density. Comparison results are shown in Table 5 and demonstrate sufficient agreement between the obtained values. Compared values have a relative deviation of 5.3 %.

This makes it possible to conclude that piezo accelerometers installed on the TO register natural longitudinal oscillations of the composite barrier. It could be assumed that the longitudinal oscillation calculated frequencies

of 524 and 604 Hz are not highlighted in the acceleration signal spectral density graphs in the form of peaks for two reasons.

1. Insufficiently high sampling rate equal to 120 Hz, when registering the acceleration signal.

2. Mutual adhesion of blocks is improved at the boundaries numbers 2 and 3 due to the screed of blocks of types 1 and 2 using beams and studs, which reduces the reflected wave amplitude at these boundaries.

Table 5

Results of comparing the frequency longitudinal oscillation values

Boundary number	Frequency calculated value, Hz	Peak frequency average value on the piezo accelerometer signal spectral density, Hz	Relative deviation, %
5	276	272.5	1.3
4	456	433.3	5.3
3	524	–	–
2	604	–	–
1	630	645.8	2.3

Obviously, no peaks at 276 and 456 Hz frequencies should be registered in collisions with a semi-infinite barrier at the test object. In order to forecast the form of a piezo accelerometer signal on the TO upon collision with a semi-infinite barrier, let us filter the signals shown in Fig. 2 by the 10-th order Butterworth blocking filters with frequency bands of 276 ± 27.6 Hz and 456 ± 45.6 Hz.

Received signals are shown in Fig. 5.

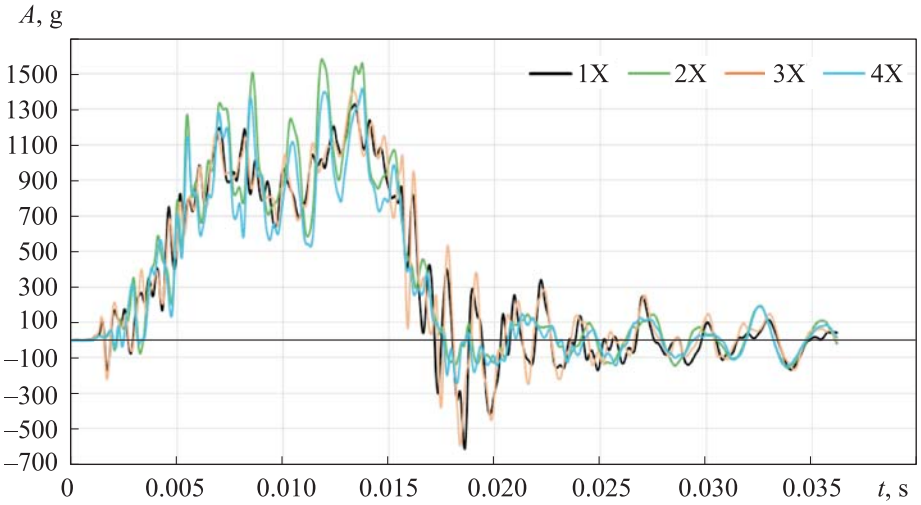

Fig. 5. Results of acceleration signal digital filtering

The A_1 peak accelerations and the τ_1 acceleration pulse duration for each piezo accelerometer signal shown in Fig. 5 are presented in Table 6. Average values of these A_{1av} and τ_{1av} parameters are also provided there.

Impact acceleration signal parameters shown in Fig. 5 are presented in Table 6.

Table 6

Impact acceleration signal parameters after filtering

Primary measurement transducer	A_1, g	A_{1av}, g	τ_1, ms	τ_{1av}, ms
1X	1329	1431	14.5	14.3
2X	1580		14.4	
3X	1402		13.9	
4X	1414		14.5	

Comparing the average values of amplitude and duration provided in Tables 2 and 6, it could be seen that acceleration amplitude after filtering decreased by 4.6 %, and duration increased by 10 %.

Conclusion. Comparison of calculated and experimental data demonstrated that the load registered on the TO interacting with a composite braking device (barrier) contains a component determined by the braking device (barrier) oscillations at natural frequencies. This should be taken into account when studying the TO reaction to shock loading, and when simulating collisions with real (semi-infinite) barriers in laboratory conditions, selecting the braking device (barrier) size and design in such a way as to minimize this component.

Translated by K. Zykova

REFERENCES

[1] Proskurin A.V. Vosproizvedenie udarnykh uskoreniy v laboratornykh usloviyakh [Laboratory reproduction of shock accelerations]. Snezhinsk, RFYaTs-VNIITF Publ., 2017.

[2] Subbotin S.G. Dinamika udarostoykikh konstruktsiy [Dynamics of shock-resistant structures]. Snezhinsk, RFYaTs-VNIITF Publ., 2003.

[3] Mogilev V.A., Novikov S.A., Faykov Yu.I. Tekhnika vzryvnogo eksperimenta dlya issledovaniy mekhanicheskoy stoykosti konstruktsiy [An explosive experiment technique for studying mechanical resistance of structures]. Snezhinsk, RFYaTs-VNIIEF Publ., 2007.

[4] Saquib D.K., Sahoo P., Srivastava A.K., et al. Performance of BLC-200 cask under 9 m drop test. *Procedia Eng*., 2017, vol. 173, pp. 455–462.
DOI: https://doi.org/10.1016/j.proeng.2016.12.063

[5] Sahoo D.K., Mane J.V., Srivastava P., et al. Numerical simulation and experimental drop testing of COCAM-120-an industrial radiography device. *Procedia Eng*., 2017, vol. 173, pp. 1918–1925. DOI: https://doi.org/10.1016/j.proeng.2016.12.252

[6] Liu X., Guo J., Bai Ch., et al. Drop test and crash simulation of a civil airplane fuselage section. *Chinese J. Aeronaut*., 2015, vol. 28, no. 2, pp. 447–456.
DOI: https://doi.org/10.1016/j.cja.2015.01.007

[7] Yeh M.K., Huang T.H. Drop test and finite element analysis of test board. *Procedia Eng*., 2014, vol. 79, pp. 238–243. DOI: https://doi.org/10.1016/j.proeng.2014.06.337

[8] Grabilin A.O., Zubrenkov B.I., Pustobaev M.V., et al. Simulating shock loading modes on spacecraft hardware at actuation of division pyro devices. *Voprosy elektromekhaniki. Trudy VNIIEM* [Electromechanical Matters. VNIIEM Studies], 2014, vol. 138, no. 1, pp. 35–42 (in Russ.).

[9] Gokhfel'd D.A., Getsov L.B., Kononov K.M., et al. Mekhanicheskie svoystva staley i splavov pri nestatsionarnom nagruzhenii [Mechanical properties of steels and alloys under non-stationary loading]. Ekaterinburg, UrO RAS Publ., 1996.

[10] Normy rascheta na prochnost' oborudovaniya i truboprovodov atomnykh energeticheskikh ustanovok (PNAE G-7-002–86) [Norms for stress calculation of equipment and pipelines for atomic power stations (PNAE G-7-002–86)]. Moscow, Energoizdat Publ., 1989.

[11] Zakharov Z.P., ed. Fiziko mekhanicheskie svoystva konstruktsionnykh materialov i nekotorye sovremennye metody ikh issledovaniya [Physical-mechanical properties of constructional materials and some modern methods of their study]. Moscow, TsNIIatomminform Publ., 1982.

[12] Chekhov A.P., Sergeev A.M. Spravochnik po betonam i rastvoram [Handbook on concrete and mortar]. Kiev, Budivel'nik Publ., 1972.

[13] Smith S.W. Tsifrovaya obrabotka signalov. Prakticheskoe rukovodstvo dlya inzhenerov i nauchnykh rabotnikov. Moscow, Dodeka-XXI Publ., 2012.

[14] Biderman V.L. Teoriya mekhanicheskikh kolebaniy [Theory of mechanical oscillations]. Moscow, Vysshaya shkola Publ., 1972.

[15] Timoshenko S.P., Goodier J.N. Teoriya uprugosti. Moscow, Nauka Publ., 1975.

Borozenets A.S. — Head of the Department, Federal State Unitary Enterprise "Russian Federal Nuclear Center — Zababakhin All-Russia Research Institute of Technical Physics" (Vasileva ul. 13, Snezhinsk, Chelyabinsk Region, 456770 Russian Federation).

Proskurin A.V. — Dr. Sc. (Eng.), Deputy Chief Design Officer, Federal State Unitary Enterprise "Russian Federal Nuclear Center — Zababakhin All-Russia Research Institute of Technical Physics" (Vasileva ul. 13, Snezhinsk, Chelyabinsk Region, 456770 Russian Federation).

Shlishevskiy A.V. — Head of the Group, Federal State Unitary Enterprise "Russian Federal Nuclear Center — Zababakhin All-Russia Research Institute of Technical Physics" (Vasileva ul. 13, Snezhinsk, Chelyabinsk Region, 456770 Russian Federation).

Please cite this article as:

Borozenets A.S., Proskurin A.V., Shlishevskiy A.V. Evaluation of the composite barrier natural oscillations influence on the generated shock loading. *Herald of the Bauman Moscow State Technical University. Series Mechanical Engineering*, 2021, no. 1 (136), pp. 103–113. DOI: https://doi.org/10.18698/0236-3941-2021-1-103-113